Investigation of Cook-Off Response Characteristics of GAP Propellant under Structural Constraints

Songlin Guo, Yi Wu, Junsen Yang, Fengkai Jin, Xingyuan Wang
School of Aerospace Engineering, Beijing Institute of Technology
Beijing, China

1 Introduction

Solid propellants are solid particle-filled polymer-based energetic composite materials, typically consisting of binders, plasticizers, metal fuels, oxidizers, and other components. Thermal loads are one of the most common and significant excitatory loads that can easily lead to safety accidents. It is extremely important to study the response process of propellants under thermal stimulation. Taking GAP propellant as an example, this paper establishes a thermal safety assessment method and experimental system for propellants under engine structural constraints. By using laser high-speed schlieren imaging to fully record the ignition, combustion, and transition to detonation of propellants under engine structural constraints, the response levels are quantitatively assessed by measuring the temperature of the propellant samples and the overpressure of the shock waves produced after detonation. The study investigates the influence of structural parameters such as casing thickness and nozzle throat diameter on the cook-off response characteristics of GAP propellants under the constraints of solid rocket motor structures.

2 Experimental Setup

The entire experimental system consists of four parts: the engine structure test piece, the temperature control system, the high-speed schlieren diagnostic system, and the pressure and temperature acquisition system, as shown in Figure 1. The structural test piece, as depicted on the left side of Figure 1, is primarily machined from aluminum alloy. A heating component is installed on the left side of the aluminum alloy structure, controlled by an electric heating rod for temperature regulation, with a controllable heating rate. A K-type thermocouple (TT-K-30-SLE) is used to monitor the temperature of the heated test piece shell in real-time. The test piece and the heater are connected by threads; once the electric heating rod is powered, it rapidly heats up, transferring heat to the heater, and subsequently to the test piece shell, thereby simulating the temperature load in the engine cook-off environment. The engine structure test piece can simulate different engine constraint structures and constraint intensities by altering the thickness of the test piece's outer mold shell and the throat diameter of the nozzle.

Correspondence to: yi.wu@bit.edu.cn

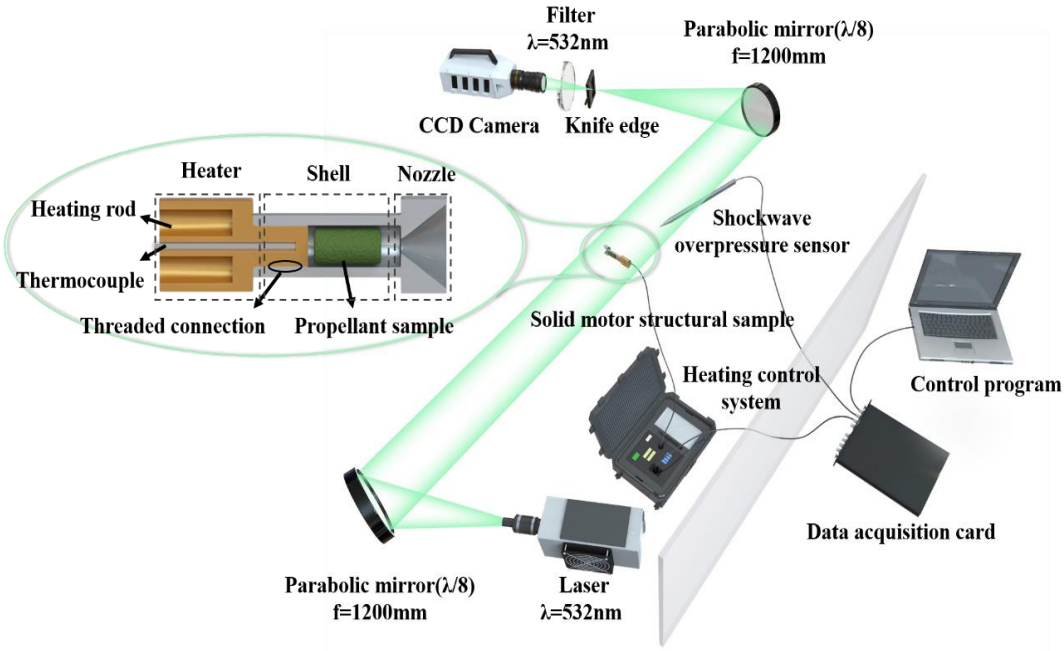

Figure 1 Schematic of the experimental setup.

This experiment employs a Z-type laser high-speed schlieren device to record the cook-off response process of the engine test piece. The device is composed of a laser, reflecting mirrors, a high-speed camera, a slit, and a filter. The laser uses a continuous 532 nm wavelength, and a slit and filter (λ=532 nm) are added in front of the camera lens, which effectively eliminates overexposure caused by the intense light from ignition and detonation. Two concave mirrors with a focal length of f=1200 mm are used, and the sample is placed between the two concave mirrors. To quantitatively assess the intensity of the thermal stimulation response, a shock wave overpressure sensor is arranged 30 cm away from the test piece to measure the overpressure of the shock wave produced after the ignition and detonation of the propellant sample. The model used is SCYG312, and the data acquisition card has a frequency of 10MHz.

The propellant used in this experiment primarily consists of 27% by mass of GAP binder, 10% by mass of RDX, 45% by mass of AP oxidizer, and 18% by mass of Al particles, as shown in Table 1.

Table 1: Component of propellant

Component	GAP	RDX	AP	Al
Content	27%	10%	45%	18%

To investigate the influence of casing thickness, nozzle throat diameter, and heating rate on the cook-off response, this study conducted a total of six experiments. The casing thickness was set to 1, 2, 3, and 4 mm, and the nozzle throat diameter was set to 1, 3, and 6 mm, as shown in Table 2.

Table 2: Measurement matrix.

Number	Shell thickness	Nozzle throat diameter	Heat flux	Heating rate
1	1 mm	1 mm	3.8×10^5 W·m^{-2}	35 ℃/min
2	2 mm	1 mm	3.8×10^5 W·m^{-2}	35 ℃/min
3	3 mm	1 mm	3.8×10^5 W·m^{-2}	35 ℃/min
4	4 mm	1 mm	3.8×10^5 W·m^{-2}	35 ℃/min
5	4 mm	3 mm	3.8×10^5 W·m^{-2}	30 ℃/min
6	4 mm	6 mm	3.8×10^5 W·m^{-2}	25 ℃/min

3 Results and Analysis

Due to the similarity in the ignition and detonation processes observed in the experiments, the schlieren images of the ignition and detonation process for the representative and distinctive Test Condition 3 were selected for analysis.

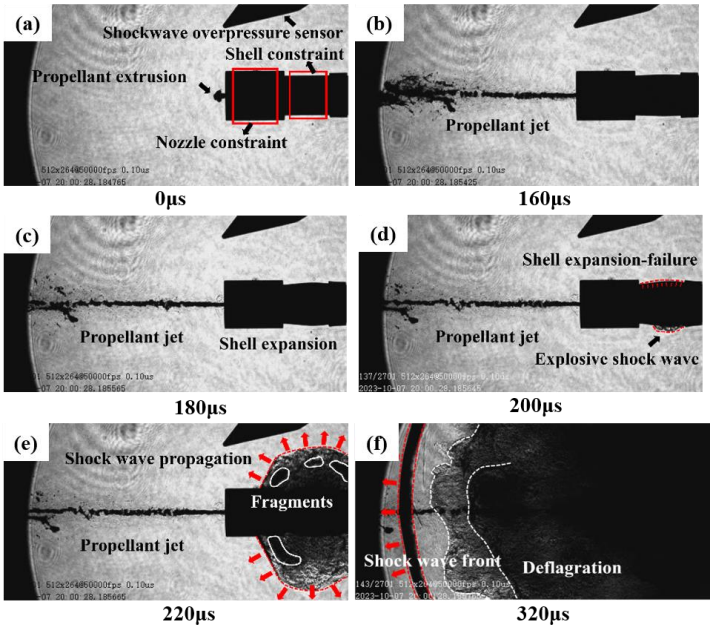

Figure 2: No.3 experiment cook off response process.

Figure 5 illustrates the ignition, detonation, and combustion propagation process of the propellant from the start to 320μs under the conditions of a casing thickness of 3mm, a nozzle throat diameter of 1mm, and a heat flux density of 3.8×10^5 W·m^{-2}, corresponding to Test Number 3. According to the schlieren images, under the action of the stimulus load, the pressure inside the confined device gradually increases, causing the propellant to be expelled through the nozzle, forming a softened, solid, mushroom-shaped jet. The jet continues to spray discontinuously until 180 μs (Figure 5 (b-c)), and the top of the jet exhibits a fluffy atomization state. Subsequently, the casing deforms and expands, as shown in Figure 5 (d), indicating a sudden increase in pressure inside the combustion chamber. By 220 μs, the casing

completely fails (Figure 5 (e)), and a large amount of propellant is ejected, resulting in a clear shock wave. Behind the shock wave, a large amount of propellant is expelled into the air, forming a detonation and combustion, as shown in Figure 5 (f). It can be seen that the cook-off response of GAP propellant under engine structural constraints is not a direct detonation but a process that successively occurs over a considerable period, involving thermal expansion, softening, ignition, combustion, and finally transitioning to detonation.

3.1 Analysis of the Influence of Casing Thickness

The summary of test results for test pieces with different casing thicknesses is shown in the table 3 below:

Table 3: Test results of different shell thicknesses

Number	Shell thickness	Nozzle throat diameter	Ignition Temperature	Ignition Time	Peak Overpressure	Shock Wave Velocity
1	1 mm	1 mm	215.9 ℃	334.1 s	0.122 MPa	765.1 m/s
2	2 mm	1 mm	214.7 ℃	324.8 s	0.174 MPa	904.1 m/s
3	3 mm	1 mm	220.8 ℃	345.4 s	0.234 MPa	791.2 m/s
4	4 mm	1 mm	222.4 ℃	311.9 s	0.249 MPa	807.3 m/s

Figure 3 illustrates the temperature changes and free-field overpressure curve changes during the test process for test pieces with different casing thicknesses.

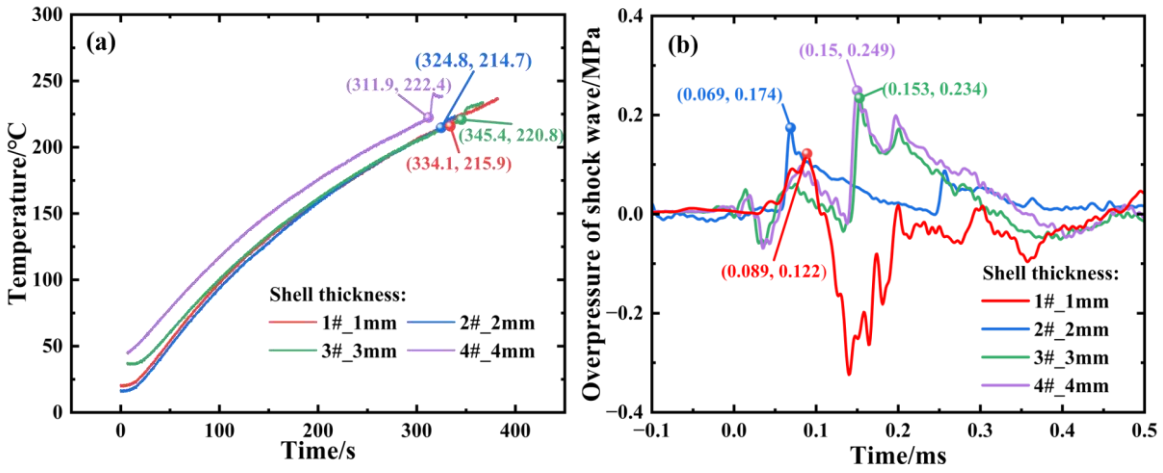

Figure 3 Comparison of (a)temperature-time curves (b)overpressure of shock wave-time curves for the GAP based propellant samples with different shell thickness.

As shown in Figure 3(a), the average ignition temperature of the tests is 218.5 °C, which suggests that the ignition temperature of the propellant under structural constraints is independent of the casing thickness. The ignition time is approximately 320 seconds, showing no significant correlation with the casing thickness. The heating rate is 35 °C/min, indicating that under the thermal load stimulation of this experiment, the propellant inside the test pieces with different casing thicknesses is heated uniformly, and there is no difference in the heating rate due to thickness variations. According to Figure 3(b), the peak explosion shock wave pressures generated during the ignition-growth-detonation process for

structurally constrained propellant test pieces with casing thicknesses of 1 mm, 2 mm, 3 mm, and 4 mm are 0.122, 0.174, 0.234, and 0.249 MPa, respectively. The peak pressure values increase with the increase in casing thickness, exhibiting a positive correlation.

3.2 Analysis of the Influence of Nozzle Throat Diameter

The summary of test results for test pieces with different nozzle throat diameter is shown in the table 4 below:

Table 4: Test results of different nozzle throat diameter

Number	Shell thickness	Nozzle throat diameter	Ignition Temperature	Ignition Time	Peak Overpressure	Shock Wave Velocity
4	4 mm	1 mm	222.4 ℃	311.9 s	0.249 MPa	807.34 m/s
5	4 mm	3 mm	225.1 ℃	366.9 s	0.056 MPa	480.20 m/s
6	4 mm	6 mm	226.1 ℃	448.2 s	0.053 MPa	469.01 m/s

Figure 5(a) displays the temperature changes during the test process for propellant structure constraint test pieces with throat diameters of 1, 3, and 6 mm. The average ignition temperature of the tests is 224.5 ℃, suggesting that the ignition temperature of the propellant under structural constraints is independent of the throat diameter. There is a clear positive correlation between ignition time and throat diameter size; the throat acts as a heat exchange channel between the propellant and the surrounding air. The larger the throat diameter, the stronger the heat exchange efficiency, which leads to a delay in ignition time.

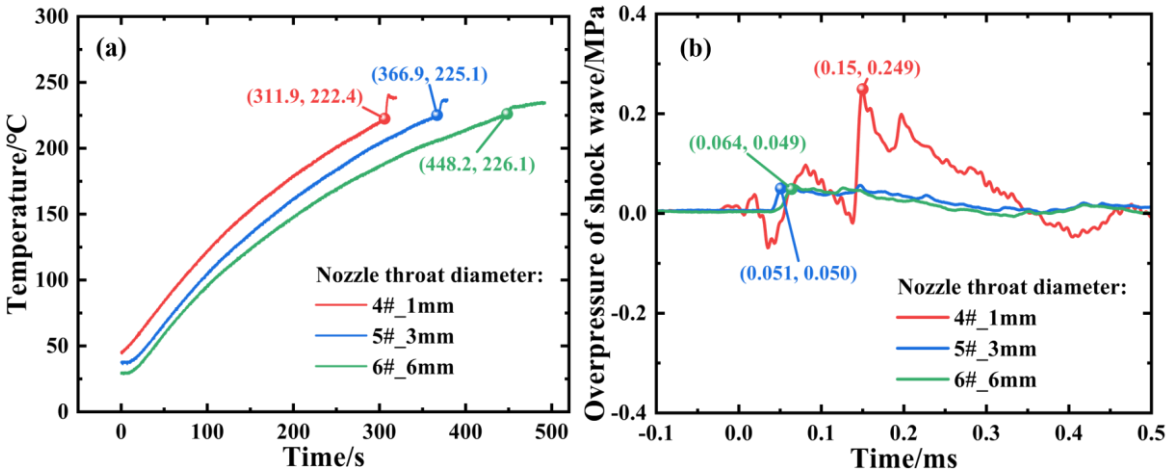

Figure 4 Comparison of (a)temperature-time curves (b)overpressure of shock wave-time curves for the GAP based propellant samples with different nozzle throat diameter

Figure 5(b) illustrates the overpressure of shock wave-time curves for the GAP based propellant samples with different throat diameters of 1, 3, and 6 mm. As can be seen from the overpressure curves, the peak explosion shock wave pressures generated during the ignition-growth-detonation process for the test pieces with throat diameters of 1 mm, 3 mm, and 6 mm are 0.249, 0.056, and 0.053 MPa, respectively. The peak pressure values decrease significantly with the increase in throat diameter, but there is no significant change in the overpressure peak values when the diameter is increased from 3 mm to 6 mm.

4 Conclusion

This paper examines the cook-off response of GAP propellant under engine structural constraints. Using high-speed laser schlieren imaging, the ignition, combustion, and detonation transition were recorded. The temperature of the propellant samples and the overpressure of shock waves post-explosion were measured. The effects of casing thickness and nozzle throat diameter on the cook-off response were studied. Key findings include:

(1) Casing thickness has minimal impact on ignition temperature but prolongs reaction time as it increases, leading to higher peak shock wave overpressure after casing failure.

(2) Ignition temperature is unaffected by nozzle throat diameter, but ignition time is positively correlated with throat size. A larger throat diameter facilitates rapid expulsion of unreacted propellant gases, preventing a high-pressure environment and reducing the intensity of the combustion-to-detonation transition by shifting some of the violent reaction to the external space.

References

[1] XIAO Bing, TIAN Xiao-tao, WANG Shao-zeng, et al. The influence of insulation layer thickness on the burning characteristics of freely loaded solid rocket engines [J]. Journal of Solid Rocket Technology, 2022(001): 045.

[2] ZHANG Hai-jun, NIE Jian-xin, WANG Ling, et al. Size effect of slow burning of hydroxyl terminated polyether propellants[J]. Acta Armamentarii, 2021(042-009).

[3] LI Xiao-dong, WANG Jing-yu, LIU Wen-jie, et al. Effect of vent hole size on combustion and explosion characteristics during cook-off tests[J]. Combustion and Flame, 2022, 240.

[4] WU Xin-zhou, LI Jun, REN Hui, et al. Comparative Study on Thermal Response Mechanism of Two Binders during Slow Cook-Off[J]. Polymers, 2022, 14(17).

[5] ZHAO Xiao-bin, LI Jun, CHENG Li-guo, et al. Study on the influencing factors of slow burning characteristics of solid propellants[J]. Chinese Journal of Energetic Materials(Hanneng Cailiao), 2011, 19(6): 4.

[6] GUPTA R, KUMAR M, SINGH S K, et al. Deflagration to Detonation Transition in Cast Explosives: Revisiting the Classical Model[J]. Propellants, Explosives, Pyrotechnics, 2022, 47(3).

[7] MOORE J S, MORRISON K D, BURNHAM A K, et al. TATB thermal decomposition: An improved kinetic model for explosive safety analysis[J]. Propellants, Explosives, Pyrotechnics, 2023.